

Investigation on Nd:YAG Laser Weldability of Zircaloy-4 End Cap Closure for Nuclear Fuel Elements

Soo-Sung Kim, Chul-Yung Lee, and Myung-Seung Yang

Korea Atomic Energy Research Institute
150 Dukjin-dong, Yusong, Taejeon, 305-353, Korea
sskim7@kaeri.re.kr

(Received July 3, 2000)

Abstract

Various welding processes are now available for end cap closure of nuclear fuel element such as TIG(Tungsten Inert Gas) welding, magnetic resistance welding and laser welding. Even though the resistance and TIG welding processes are widely used for manufacturing commercial fuel elements, they can not be recommended for the remote seal welding of a fuel element at a hot cell facility due to the complexity of electrode alignment, difficulty in the replacement of parts in the remote manner and a large heat input for a thin sheath. Therefore, the Nd:YAG laser system using optical fiber transmission was selected for Zircaloy-4 end cap welding inside hot cell.

The laser welding apparatus was developed using a pulsed Nd:YAG laser of 500 watt average power with optical fiber transmission. The weldability of laser welding was satisfactory with respect to the microstructures and mechanical properties comparing with TIG and resistance welding. The optimum operation processes of laser welding and the optical fiber transmission system for hot cell operation in a remote manner have been developed. The effects of irradiation on the properties of the laser apparatus were also being studied.

Key Words : Nd:YAG laser welding, TIG welding, zircaloy-4, optical fiber

1. Introduction

Various studies have been actively conducted for developing a new nuclear fuel and manufacturing a capsule for its irradiation test. In such studies, remotely controlled welding work has been required to be performed in a highly radioactive hot cell for manufacturing the nuclear fuel. [1,2] Meanwhile, the laser has been considered for remotely controlled welding work, since the optical

fiber transmission system is easy for laser welding in a shielded facility. But there is also a technical challenge of securing a higher welding quality in the laser welding work. According to the process of manufacturing nuclear fuel, the end cap welding of the fuel element is to weld a Zircaloy-4 cladding tube, which is charged with pellets, with the end cap. Such end cap welding requires high reliability, since if there is a defect in only one single point along the circumference of the fuel element

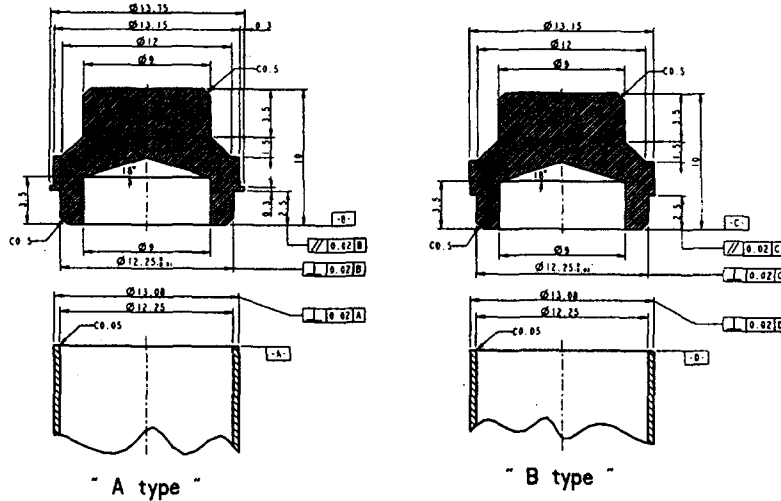


Fig. 1. Configuration of Zircaloy-4 Weld Specimens

Table 1. Chemical Compositions and Mechanical Properties of Zircaloy-4

Chemical compositions				
Element	Sn	Fe	Cr	Zr
wt. %	1.2-1.70	0.18-0.24	0.07-0.13	Bal.
Mechanical properties				
Tensile strength (kpsi)	Yield strength (0.2% offset, kpsi)		Elongation (%)	
63.8	50.1		32.0	

welding, it will cause the radioactive fission products to leak out during combustion of the nuclear fuel, and consequently bring about serious safety problems. [3] This study was conducted to develop the optimum conditions for the remote laser welding system and to evaluate the performance of the weld zone in sealing of the Zircaloy-4 end cap of the nuclear fuel element.

2. Experimental Procedure

2.1. Materials

The parent material used in this study was

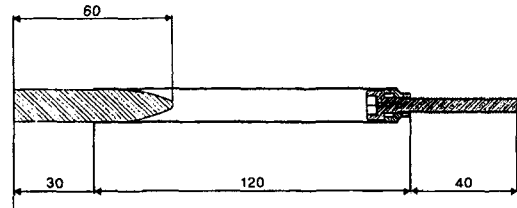


Fig. 2. Zircaloy-4 Tube Specimen Used in the Tensile Test

Zircaloy-4. The chemical composition, mechanical properties and the configurations of test specimens are given in Fig 1 and Table. 1, respectively. These specimens were welded for their end caps and cladding tubes. From the laser and TIG welded samples, tensile specimens were machined as shown in Fig. 2. These specimens were ultrasonically cleaned in ethyl alcohol, and dried.

2.2. Laser Welding Equipment

The remotely controlled welding chamber was manufactured as shown in Fig. 3 using the Nd:YAG laser system with an optical fiber

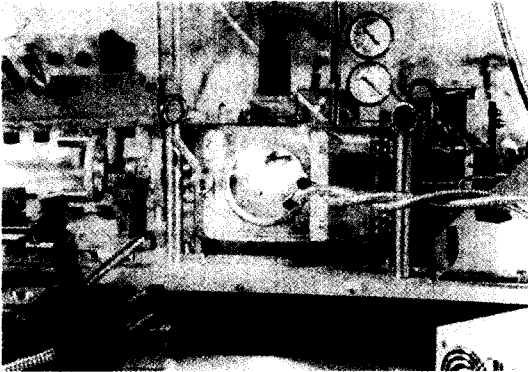


Fig. 3. Photograph of the Welding Chamber with an Optical Coupler

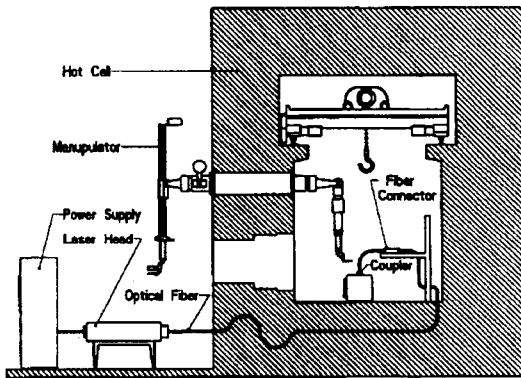


Fig. 4. Schematic Illustration of the Optical Fiber Delivery System in a Hot Cell

transmission system in order to weld the end cap of the nuclear fuel element in a hot cell. The welding chamber is comprised of a body, a rotary driving section, an end cap inserting section, an optical fiber and a coupler section. When the beam oscillating from the laser system is transmitted, the optical fiber, which is very flexible, thin and long, is utilized for transmission. Since the distance between the welding stage in the hot cell and the laser system outside the hot cell was about 20m, an optical coupler was required to connect the welding chamber with the optical fiber. As illustrated in Fig. 4, the optical coupler was manufactured in such a way that it enabled

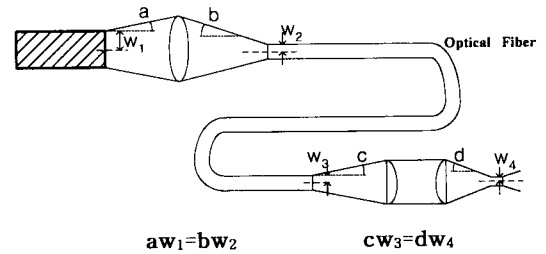


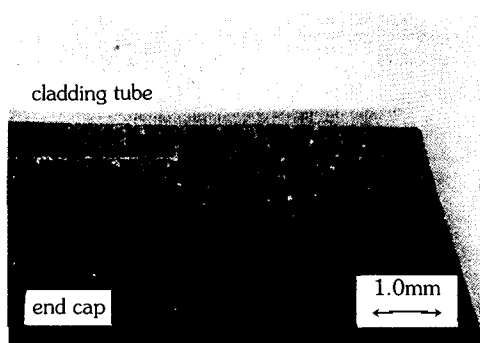
Fig. 5. Conservation of Laser Beam Quality Using the Optical Fiber

the optical fiber, the optical fiber connector and the coupler to be replaced easily.

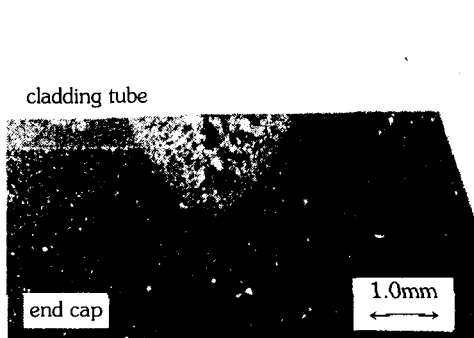
2.3. Fiber Transmission System

If the beam emitting from the Nd:YAG laser system is directly casted, its degree of positional freedom becomes poor and it is inconvenient to use the beam in a narrow space. Therefore, the flexible, thin optical fiber is used.

In focusing the laser into optical fiber, the beam quality is conserved as illustrated in Fig. 5. In the fiber transmission, the focusing angle (b) is conserved under certain circumstances. Small focusing optics and working distances are obtained for small beam quality factors. The optical fiber transmission system is comprised of an optical inlet coupler, an optical fiber and an optical outlet coupler. The optical inlet coupler is a section where the beam is connected with an internal part of the core of the optical fiber by an incident lens. The optical fiber, which is a quartz glass of pure SiO_2 , is comprised of a core part having a wide refractive index and a cladding part having a narrow refractive index, whose diameters of the core are 600, 800 and 1000 μm , respectively. This SI (Step Index) is multi-mode type, and the NA (Numerical Aperture) of the optical fiber is 0.22. The focusing lens of the coupler as used is of UV grade fused silica.



(a) Macrostructure of TIG Welding



(b) Macrostructure of Laser Welding

Fig. 6. Comparison of TIG and Laser Weldment

2.4. Mechanical Test & Metallography

Tensile testing of the specimens accomplished under ASTM standard E8 using an Universal testing machine. The crosshead speed for test specimens was 0.001/s in gauge length 25mm. A series of Vickers hardness numbers was taken across several welded specimens. Microhardnesses were determined under a 100 g load at 0.2mm intervals across the weld, through the HAZ(Heat Affected Zone), and into the base metal. Areas of material selected for microscopic examination were mounted in Buehler resin. Specimens were polished then etched with the following etchants : H₂O 45%, HNO₃ 45%, HF4 10% were taken to show the overall weld area followed by the polaroid (X200) to show weld, HAZ, and base

metal microstructure. Finally, the amounts of ZrO₂, which have fumes on the protective glass, were measured by the micro -electro balance.

3. Results and Discussion

3.1. Evaluation of Welding Performance

The geometric joint configuration of end cap and tube has a significant effect on end cap welding. Any improvement in the geometry of the welding joint is of advantage to the autogenous process. If solidification is brought about only in one direction during welding, it can be easy to melt it. Usually, laser welding causes a molten pool in the material more easily than TIG welding, and a deep weld penetration can be made by laser welding. Fig. 6 shows a typical sectional view of TIG welding and laser welding in the end cap welding of the Zircaloy-4 cladding tube. As shown in Fig. 6, laser welding was found to have a much smaller HAZ, comparing with TIG welding. Moreover, TIG welding usually had a larger melting volume, compared with laser welding which melts by high density energy.

3.2. Characteristics of Laser Beam Transmission by Fiber Connector

Considering the high radioactivity in the hot cell, the optical fiber connector was developed to be installed in the upper part of the welding chamber so that contaminated optical fiber could be immediately replaced with a new one by the remote control as shown in Fig. 4. Moreover, the optical fiber from the optical inlet coupler outside the hot cell to the optical fiber connector inside the hot cell is fixed, and the optical fiber is to be replaced when it is contaminated. In this study, an optical fiber of dia. 600 μ m was used from the laser head to the optical fiber connector, and an

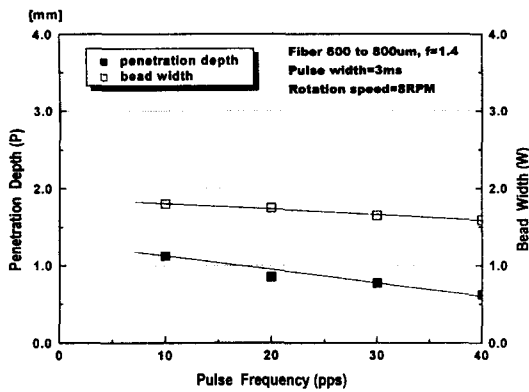


Fig. 7. Relationship Between Penetration and Pulse Frequency Using Fiber of 600 to 800 μm

optical fiber of dia. 800 μm and another optical fiber of dia. 1000 μm were used from the optical fiber connector to the optical outlet coupler, respectively. The reason is the beam focused on the collimating lens had to be within the largest allowable range in consideration of the characteristics of the law of beam quality preservation. The welding experiment was conducted under the following conditions : the optical outlet coupler representing the optical fiber of dia. 800 μm , $F\#=2$, focal length of the condenser $FL = 95$ mm or 120 mm, and the optical factor = 1.4 or 2.1. Fig. 7 shows the relationship between the weld penetration and pulse frequency using the 600 to 800 μm optical fiber at $FL=95$. In the case of optical factor = 1.4, the weld penetration was found to be greater at $FL = 95$ mm than $FL = 120$ mm. In the case of the optical factor = 2.1, the bead was found to be 1.8 mm at $FL = 120$ mm, which was wider than that $FL = 95$ mm by 0.3 ~ 0.4 mm. In the case of $FL = 95$ mm and an optical fiber of dia. 600 μm , the weld penetration was found to be deep. In the case of $FL = 120$ mm and an optical fiber of dia. 1000 μm , the width of the bead was found to be the greatest width of 2.2mm.

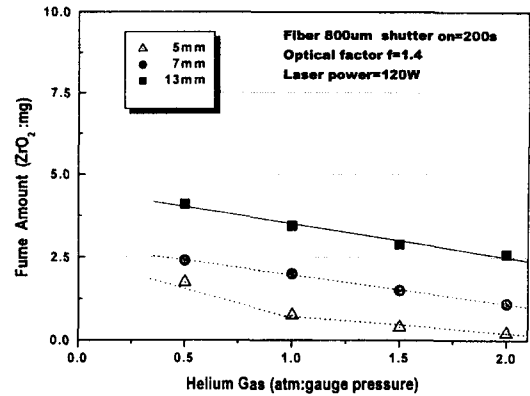


Fig. 8. Effect of Fume Amount on the Gas Pressure of Helium

3.3. Influence of Assistant Gas and the Nozzle of the Outlet Coupler

When the laser beam reaches the material surface, plasma is formed causing a plume to be generated. Moreover, when the laser beam irradiates the material surface, a metal vaporization reaction is generated on the surface. Therefore, it has to be considered in laser welding that such a reaction is likely to cause some damage to the condenser. This reaction raises serious considerations regarding the pressure of the assistant gas to be used for blowing away the plume, the diameter of the nozzle of the optical outlet coupler, the angle of incidence of the coupler and the distance between the material and the nozzle. Also, the assistant gas and the plume phenomenon have a very close relationship in the welding process, and have great influence on the welding qualities. This laser welding experiment was conducted under the following conditions : the optical outlet coupler representing a 50 LPM(liter/min.) primary flowrate of helium (the flowrate of helium inside the nozzle), a 12 mm distance between the material and the nozzle, and

Table 2. Tensile Properties of TIG and Laser Welded Specimens

Specimen Type		Dimension		0.2% YS (ksi)		UTS (ksi)		% E in 50mm	
				Each	Ave.	Each	Ave.	Each	Ave.
TIG welding	A	13.08 × 12.24 (O.D) (I.D)	62.5	62.9	78.4	78.4	37.2	37.1	
			65.5		80.1		35.6		
			60.8		76.8		38.5		
	B		58.9	59.2	75.4	76.7	35.7	36.3	
			61.4		77.1		36.5		
			57.4		77.6		36.7		
Laser welding	A		57.5	61.3	75.3	75.4	40.2	39.7	
			65.1		77.1		39.4		
			61.3		73.8		39.4		
	B		57.7	61.9	77.6	77.5	36.2	37.3	
			66.3		78.3		35.8		
			61.8		76.5		39.9		

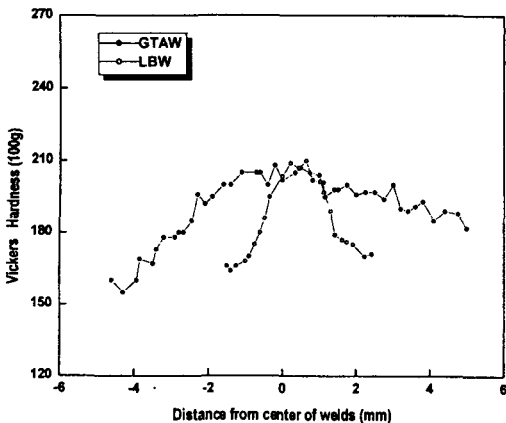


Fig. 9. Variations in the Microhardness Along the Sheath-HAZ-endcap in TIG and Laser Welding

a 7 mm nozzle diameter. Fig. 8 shows the effect of the amount of fumes on the gas pressure of helium. When the secondary pressure of helium (gauge pressure), while helium was blown horizontally from the nozzle inlet, increased from 0.3 atm to 1.4 atm, oxide zirconium was found to slightly cling to the condenser. However, when it exceeded 2 atm, the bead of the material surface

was found to be rough due to the boiling phenomenon. Accordingly, it is judged that if the primary flowrate of helium at the optical outlet coupler is 50LPM, the secondary pressure thereof shall be at least in the range of 1 atm to 1.4 atm.

3.4. Mechanical Test

The hardness test was conducted for the base metal, HAZ, and the weld metal by a Vickers hardness tester. Fig. 9 comparatively shows the results for the specimens welded by TIG and laser welding. In the TIG welded specimen and laser welded specimen, the hardness of the weld metal was found in the range of 180 to 210, and the hardness of HAZ between the weld metal and the base metal was found to be in the range of 160 to 180. The difference in the hardness of the weld metal between the laser and TIG welded specimens were not so great. In both the TIG and laser welded specimens, the closer the test zone of the end cap sample was to the edge, the higher the hardness was found, as being a little higher than that of the cladding tube. It is therefore

Table 3. Burst Properties of TIG and Laser Welded Specimens

Specimen Type		Dimension	UBS (MPa)		UBE (%)	
			Each	Ave.	Each	Ave.
TIG welding	A	13.08 × 12.24 (O.D) (I.D)	530	528	28.8	28.5
			527		26.4	
			528		30.2	
	B		532	527	28.9	28.2
			524		27.5	
			525		28.1	
Laser welding	A		524	526	39.9	37.8
			526		36.2	
			528		37.2	
	B		530	525	30.7	35.4
			520		37.6	
			522		37.8	

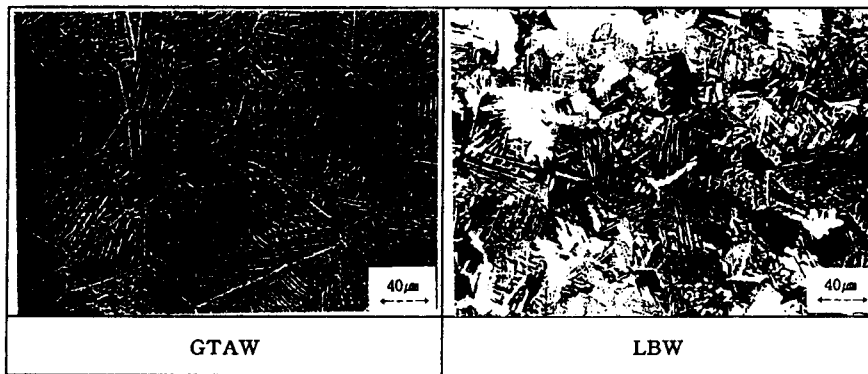


Fig. 10. Variations in the Microhardness Along the Sheath-HAZ-endcap in TIG and Laser Welding

judged that the hardness was high because the weld zone of the end cap became abruptly cold from the overheating condition by the heat cycle. Also, the weld metal and HAZ area of the laser welded specimens were found to be narrower, compared to the TIG welded specimens.

Table 2 comparatively shows the yield strength, tensile strength and elongation obtained from tensile tests depending on the differences in the geometrical configurations of the TIG and laser

welded specimens, i.e., A geometry (specimen with filler part) and B geometry (specimen without filler part). The tensile strength of the TIG welded specimens and that of the laser welded specimens were higher than that of the base metal. The elongation of laser welded specimens tended to be a little higher than that of the TIG welded specimens. There was also little difference in yield strength and elongation between the A and B geometry samples, and their tensile strengths were

found to be similar. When the burst tests were examined, the ultimate burst elongation of laser welded specimens was found to be 36% on average, which was much higher than that of the TIG welded specimens. Also, in terms of the geometrical configuration of the Zircaloy-4 weld zone, the mean value of the ultimate burst elongation of the A geometry sample was found to be high. Table 3 comparatively shows the ultimate burst strength and the ultimate burst elongation obtained from the seal burst test.

3.5. Microstructure Examination

Since the weld zone is locally heated and cooled to the extent of its phase boundary areas or even beyond them according to the welding parameters, the weld zone experiences different phase transformations to have various microstructures.[4] It was observed that while the α grains in the microstructure of the base metal cladding tube were longitudinally elongated, the microstructure of the base metal region of the end cap was of an irregular structure with equiaxised, recrystallized α grains. The microstructures show a typical form where the phase in the prior β grain smaller than that in weld metal region grew to be plate form. The observed HAZ shows that most of the α grains were transformed, and that the HAZ was heated to the extent of the $\alpha+\beta$ phase area and thereafter the grains grew to be of irregular forms and sizes.

The microstructures of the weld metal regions of the TIG and laser welding are shown in Fig. 10. While the weld metal region of TIG welding appears to be very similar to the quenched structure, where prior grains grew greatly, and the weld metal region of laser welding appears to have a relatively small size of prior grains.[5] This phenomenon seems to result from the fact that in the case of laser welding, the absorbed heat

energy was locally less than that of TIG welding, because in laser welding the welding time is short and the cooling rate is very fast. Accordingly, the weld metal region of the weld zone of the Zircaloy-4 end cap appears to be of a mixed structure, where the martensitic α' structure and the Widmanstatten α phase in the prior β grain are intermixed due to relatively fast heating and cooling rates.

4. Conclusions

This study was conducted to develop a remote Zircaloy-4 end cap welding, utilizing the Nd:YAG laser system including optical fiber transmission. The welding performance is evaluated as follows.

- 1) As a result of examining the characteristics of laser welding by optical fiber transmission, in the case of optical factor = 1.4, the weld penetration was found to be greater at FL = 95 mm than FL = 120 mm. In the case of optical factor = 2.1, the bead width was found to be 1.8 mm at FL = 120 mm, which was wider than that of FL = 95 mm by 0.3 ~ 0.4 mm.
- 2) The secondary pressure of helium (gauge pressure) at the optical outlet coupler, when laser welding was performed, increased from 0.3 atm to 1.4 atm, and oxide zirconium was found to slightly cling to the condenser. When the primary flowrate of helium at the optical outlet coupler was 50LPM, the secondary pressure thereof shall be at least in the range of 1 atm to 1.4 atm.
- 3) When the Zircaloy-4 end cap weld zone was observed, laser welding zone was smaller than the TIG welding zone, and the microstructure of the weld zone in both the TIG and laser welded specimens appeared to be of a mixed structure, where the martensitic α' structure and the Widmanstatten α phase in the prior β grains were intermixed.

4) In the mechanical test of the Zircaloy-4 end cap weld zones, both processes were found to have good results, but the weld zone using the laser welding process was found mostly to have a greater weld penetration than that of the TIG welding process, and further to have good weldabilities with the formation of fine grains.

Acknowledgements

This work was carried out under the 'Long-term Nuclear R&D Program' supported by the Ministry of Science and Technology of the Republic of Korea.

References

1. J. Saito, M. Shimizu, "Development of Re-instrumentation Technology for Irradiated Fuel Rod", The 2nd Kaeri-Jaeri Joint Seminar on PIE Tech., KAERI-NEMAC/TR-32, 125-135, (1995).
2. H. Sakai, H. Kawamura, "New Apparatus of JMTR Hot Laboratory", Department of JMTR, The 2nd Kaeri-Jaeri Joint Seminar on PIE Tech., KAERI-NEMAC/TR-32, 65-77, (1995).
3. P. T. Truant, "CANDU Fuel Performance & Power Reactor Experience", AECL-MISC-250-3 Rev.1, (1983).
4. R. A. Holt, "The Beta to Alpha Phase Transformation in Zircaloy-4", Journal of Nucl. Mat., 35, 322-325, (1995).
5. V. RAM, G. KOHN & A. STERN, "CO₂ Laser Beam Weldability of Zircaloy 2", Welding Journal, July, 147-151, (1986).